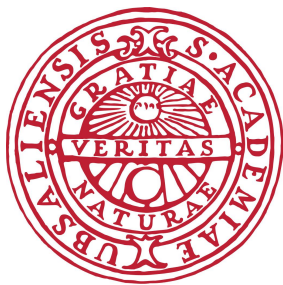


Master's Programme in Physics, specialising in Nuclear and Particle Physics

Advanced Physics - Project Course, 10 credits, (1FA565)

---

# Development of an event generator for antihyperon-hyperon pair production in antiproton-proton collisions



Uppsala University

Department of Physics and Astronomy

Division of Nuclear Physics

Author: Vitor José Shen <sup>†</sup>

Supervisor: Michael Papenbrock

June 30, 2022

---

<sup>†</sup>vitor-jose.shen@physics.uu.se

---

# Abstract

The goal of this project was to develop a lightweight Monte-Carlo (MC) event generator for hyperon pair production in antiproton-proton collisions, and demonstrate it in one of the hyperon decay reaction channels , which is  $\bar{p} + p \longrightarrow \bar{\Lambda} + \Lambda \longrightarrow \bar{p}\pi^+ + p\pi^-$ . The prototype of this external MC event generator we presented here is based on the software framework of ROOT. Compared to the corresponding framework of embedded MC event generators that is currently used in the PANDA experiment at FAIR, PandaRoot, it allows for easier and quicker testing of new models or formalisms on synthetic data, for example for studying spin observables like polarisation. The event generator was benchmarked by studying angular distributions in final states, which are constructed by kinematic relations of 4-momentum vectors in different reference frames for all mother and daughter particles.

**Key words:** MC event generator, Antihyperon-hyperon pair, Antiproton-proton collisions, PANDA, ROOT, 4-vector kinematics, Angular distribution

# Table of Contents

<b>Abstract</b>	<b>I</b>
<b>1 Introduction</b>	<b>1</b>
1.1 Hyperon Physics and $\bar{p}p$ collisions . . . . .	2
1.2 $\bar{\Lambda}$ PANDA experiment at FAIR . . . . .	3
1.2.1 FAIR . . . . .	3
1.2.2 $\bar{\Lambda}$ PANDA . . . . .	4
1.3 The current tools for simulation and analysis: PandaRoot . . . . .	5
1.4 Event Generator . . . . .	6
1.4.1 Background . . . . .	6
1.4.2 The External Event Generator developed in this project . . . . .	6
<b>2 Methodology</b>	<b>7</b>
2.1 4-Vector Kinematics . . . . .	8
2.2 Hyperon and Anti-hyperon Rest Frame . . . . .	10
2.3 $\bar{p}p$ Centre of Mass Frame . . . . .	10
2.3.1 Lorentz Boost . . . . .	10
2.3.2 Rotation . . . . .	11
<b>3 The framework and output results of the External Event Generator</b>	<b>13</b>
3.1 ROOT Tree format . . . . .	13
3.2 Test for uniform distribution . . . . .	15
3.3 Generation of physics quantities . . . . .	16
3.3.1 Angular distribution in hyperon and antihyperon rest frame . . .	16
3.3.2 Angular distribution in $\bar{p}p$ CM frame . . . . .	17
3.3.3 Angular distribution in $\bar{p}p$ CM frame after rotation . . . . .	20
3.3.4 Angular distribution in hyperon and antihyperon rest frame after rotation . . . . .	22
<b>4 Conclusion &amp; Outlook</b>	<b>24</b>
<b>Reference</b>	<b>25</b>

# 1 Introduction

The event generators for the PANDA [1] experiment at FAIR [2] are currently embedded into its software framework, PandaRoot [3]. While this can be very convenient for the PandaRoot user when running a full Monte Carlo simulation, it is also very resource-demanding. Furthermore, it requires compiling a large software package with a complex dependency tree. Thus, it becomes a difficult task to quickly test new models and formalisms on synthetic data, especially for those study topics about spin observables of hyperons decay. For instance, for  $\Lambda \rightarrow p\pi^-$ , there is a relation [4] to reconstruct the polarisation of the mother hyperon by measuring the angular distribution of the proton:

$$I(\cos\theta_p) = \frac{1}{4\pi}(1 + \alpha_\Lambda P_n \cos\theta_p) \quad (1.1)$$

where  $I(\cos\theta_p)$  is the angular distribution of the cosine of the polar angle of the decay proton,  $\alpha$  is a decay parameter of  $\Lambda$ , and  $P_n$  is a polarisation component, see [4] for details. Being able to easily test different models for these processes, which in turn manifest in different angular distributions, corresponds to the goal of this project.

This issue was addressed in this project by developing a lightweight event generator for hyperon pair production in antiproton-proton collisions, and mainly demonstrated in the specific reaction channel of  $\bar{p} + p \longrightarrow \bar{\Lambda} + \Lambda \longrightarrow \bar{p}\pi^+ + p\pi^-$ .

The process requires generating angular distributions for the final state particles in the hyperon rest frame as well as calculating their absolute momentum from the mass difference of the hyperon and its daughter particles. From the generated quantities the 4-momentum vectors will be constructed and then transformed into the center-of-mass frame of the reaction.

The physics background and software tools involved in this project are presented in this introductory chapter 1, including the specific properties of hyperons, a brief introduction to the PANDA experiment at FAIR, as well as a brief introduction to ROOT [5], FairRoot [6], PandaRoot, and the general concept of event generators. The relations of 4-vectors kinematic as the methodology to construct the event generator are introduced in chapter 2. The framework of this external event generator and its discussion are presented in chapter 3 of this report. A conclusion and outlook are given in the final chapter 4.

## 1.1 Hyperon Physics and $\bar{p}p$ collisions

A branch of physics research and studies that concerns hyperons, is called strangeness physics. Broadly speaking, it is related to the fields of hadron physics, nuclear physics, and astrophysics.

The objects studied, hyperons, are subatomic particles in the category of matter called baryons. From the point of view of constituent quarks, they are similar to the more commonly known baryons, i.e., the protons and neutrons. If we make a comparison of hyperons with protons and neutrons, they all have three quarks. But the main difference is that, unlike protons and neutrons which contain only up (u) quarks or down (d) quarks, the hyperons contains at least one strange (s) quark, and sometimes a charm (c) quark as well (The latter is usually called charmed hyperon in order to distinguish).

In other words, what we are referring is to the case that at least one of the up or down quarks is replaced by a strange quark in the case of neutron or proton. That is, the baryons that contain strange quarks are of interest in this branch of physics research.

The letters  $Y$  and  $\bar{Y}$  are usually used to denote hyperons and anti-hyperons, respectively.

$Y$	$q$	$c\tau$ (cm)	$\tau(s)$	$M$ (GeV/c $^2$ )	Decay
$\Lambda$	uds	7.89	$2.632 \times 10^{-10}$	1.116	$p\pi^-$ (63.9%)
					$n\pi^0$ (35.8%)
$\Sigma^+$	uus	2.404	$8.018 \times 10^{-11}$	1.189	$p\pi^0$ (51.57%)
					$n\pi^+$ (48.31%)
$\Sigma^0$	uds	$2.22 \times 10^{-9}$	$7.4 \times 10^{-20}$	1.193	$\Lambda\gamma$ (100%)
$\Sigma^-$	dds	4.434	$1.479 \times 10^{-10}$	1.197	$n\pi^-$ (99.848%)
$\Xi^0$	uss	8.71	$2.0 \times 10^{-10}$	1.315	$\Lambda\pi^0$ (99.524%)
$\Xi^-$	dss	4.91	$1.639 \times 10^{-10}$	1.322	$\Lambda\pi^-$ (99.887%)
$\Omega^-$	sss	2.461	$8.21 \times 10^{-11}$	1.672	$\Lambda K^-$ (67.8%)
					$\Xi^0\pi^-$ (23.6%)
					$\Xi^-\pi^0$ (8.6%)

Table 1.1: Strange ground state hyperons. The name of hyperon, its quark content, mean decay length, mean lifetime, mass, and main decays with branching ratio are shown, and they are denoted by  $Y$ ,  $q$ ,  $c\tau$ ,  $\tau$ ,  $M$ , and Decay. Data from [7].

A list of ground-state hyperons and their properties is summarised above in Table 1.1.

The  $\Lambda$  hyperon, is the lightest in mass among hyperons. As can be seen from Table 1.1, many of the heavier hyperons have dominant decay chains including the  $\Lambda$ . It is also a relatively long-lived hyperon, which means with its mean decay length at the speed of light  $c\tau = 7.89$  cm, in typical experiments, it will travel a measurable distance between

the point of creation and decay.

In general, since hyperons contain at least one strange quark, it is much heavier in mass. Many hyperons have been studied in great details. However, especially for hyperons containing more than one strange quark, there have been few opportunities to do that in  $\bar{p}p \rightarrow \bar{Y}Y$ .

Some physics puzzles might be figured out through the studies of hyperons. For example, the question about the matter-antimatter asymmetry in the Universe can be connected to hyperon spin observables through the violation of conservation charge symmetry and parity, i.e., CP violation. Or the so-called hyperon puzzle, related to the presence of strange quarks (or hyperons) in the inner core of neutron star, i.e., described by the Equation of State (EoS) with hyperons, may possibly be a solution to this question.

There are several possible ways to produce pairs of hyperons. One of them would be using anti-proton proton collisions (annihilation), since it provides a larger cross section to produce anti-hyperon hyperon pairs [1], when compared to other possibilities like production from positron-electron collisions.

## 1.2 **PANDA experiment at FAIR**

The PANDA Experiment will be one of the key experiments at the Facility for Antiproton and Ion Research (FAIR) which is under construction and currently being built on the area of the GSI Helmholtzzentrum für Schwerionenforschung in Darmstadt, Germany.

### 1.2.1 FAIR

"FAIR" stands for "Facility for Antiproton and Ion Research in Europe".

Four experiment pillars can be subdivided from FAIR-GSI, including PANDA. The central part of FAIR is an accelerator complex providing intense pulsed ion beams (from p to U). Antiprotons produced by a primary proton beam will then be filled into the High Energy Storage Ring (HESR) which collide with the fixed target inside the PANDA Detector.

Refer to Figure 1.1 in the next page, there are planned facilities (highlighted in red colour) that are being built, and the existing accelerator facilities (highlighted in blue colour) will also become part of FAIR and will serve as first acceleration stage.

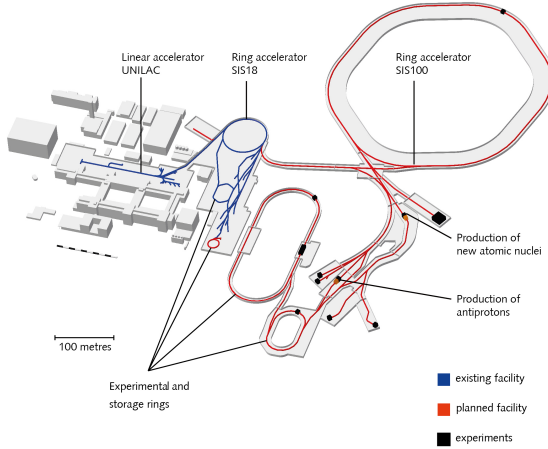


Figure 1.1: The new accelerator facility of FAIR [2], which is now under construction

### 1.2.2 $\bar{\text{P}}\text{ANDA}$

The acronym " $\bar{\text{P}}\text{ANDA}$ " or "PANDA" stands for "antiProton ANihilation at DArmstadt". A schematic overview of the PANDA spectroscopy with the 3D sliced view, that can see through the inner structure of the proposed detector, is shown in Figure 1.2. The design goal for detector is to provide a nearly full coverage of the solid angle together with good particle identification and high energy and angular resolutions for charged particles and photons. From Figure 1.2, we can tell that, the proposed detector can be subdivided into different components by their functioning.

- The various tracking detectors that are labelled in red colours
- The particle identification (PID) components which are labelled in blue colours
- The electromagnetic calorimeters which are labelled in green
- The cluster jet / pellet target system which is labelled in black

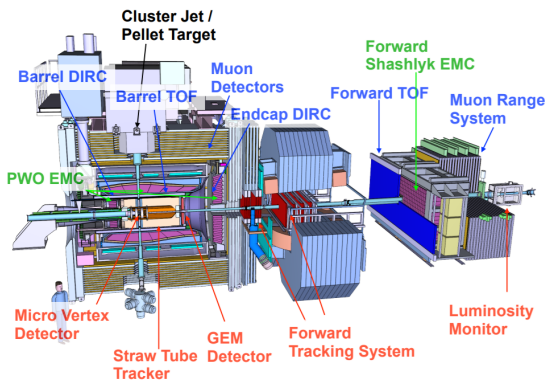


Figure 1.2: The schematic overview of the PANDA detector spectroscopy [1]

### 1.3 The current tools for simulation and analysis: PandaRoot

The simulation and reconstruction software package for the PANDA experiment is called PandaRoot, which is initially based on the framework of FairRoot, as the latter one is mainly developed for the future experiments at FAIR. One can also notice that they are built on the open-source data analysis framework called ROOT which is frequently used in HEP, Nuclear physics, and other disciplines.

The first PandaRoot simulation-reconstruction chain was successfully tested on the PANDA Grid in February 2007. The structure of the software reflects the Monte-Carlo simulation chain as it is illustrated in Figure 1.3 below.

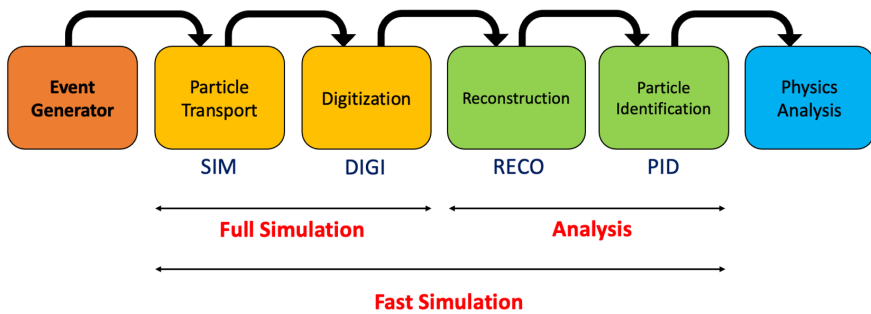


Figure 1.3: Simulation stages within the framework of PandaRoot

Referring to figure 1.3, the basic idea is that there are 6 main stages in the framework of simulation-reconstruction chain [8] in PandaRoot.

The first and the starting point in the simulation stage, the embedded event generators within PandaRoot. They can specify the initial state particle distributions, physics channels and antiproton-proton background reactions, with several complementary event generators that can be selected by user, including EvtGen [9], DPM [10], UrQMD [11], and Pythia [12]. In the following stage, the particle transport through the detector material is simulated with Virtual Monte Carlo, Geant4 [13] or Geant3 [14]. Then it comes to the digitization stage, the generated MC data is processed to simulate the realistic response of the subdetectors. For the reconstruction stage information provided by the tracking detectors are combined to reconstruct charged tracks and propagate these to the outer subdetectors. For the PID part, probability density functions (p.d.f.) are computed for every track based on different detectors and various particle identification (PID) concepts. It ultimately goes to physics analysis stage, various fitting algorithms for the four momentum and position of the particles as well as particle selection and combination mechanisms are provided.

## 1.4 Event Generator

As discussed in section 1.3, the event generator is the first part in the structure framework of simulation chain of PandaRoot. The light-weight event generator which we are developing, built on ROOT as a external event generator, as a different approach compared to the original embedded event generator in PandaRoot. In order to satisfy the purpose and need of fast-testing formalisms and models for polarisation or other spin observables studies on  $\bar{Y}Y$  from  $\bar{p}p$  annihilation.

### 1.4.1 Background

The Monte Carlo (MC) Event Generator, or in this report just simply refer it as "event generator", is the part of the software that produces the information of physical quantities of particles in the final state. It provides input for the MC simulation chain and is usually followed by the simulated particle transport through the detector material.

In general, the Monte-Carlo Event Generator, can be considered as the software which produces particles in final states for MC simulation. It simulates decay chains, angular distributions, 4-momenta, initial positions, and particle identities. Then they are passed to transport engine which simulates the interaction of particles from event generator with material of detector.

### 1.4.2 The External Event Generator developed in this project

An external event generator, as its name suggested, can be compiled and run standalone. It is lightweight, easy to modify, and has few dependencies.

Normally, for the whole matured software framework for the simulation and analysis, the way of embedded is used without many issues. This approach is convenient, because the generator can be called directly by the simulation script and be run together with the transport code. However, the output information is not stored in a separate file. Also, when running the same events again, the event generator has to reproduce them.

An external event generator can complement this setup. It produces the output events file independently, generates events once and then passes them to the particle transport code. The most important feature here that we are considering is, we want to input angular distributions that have been obtained from physics models. In embedded event generators, the ability to modify the angular distributions of particles in different steps of the decay chain can be limited. Therefore, the goal is to provide a more convenient way to provide custom inputs to these distributions.

## 2 Methodology

The new algorithm should generate 4-vectors for  $\bar{\Lambda}\Lambda$  pair, including their  $p\pi^-$  and  $\bar{p}\pi^+$  decay products, from  $\bar{p}p$  annihilations. We can first generate the angular distribution of  $p\pi^-$ , and  $\bar{p}\pi^+$  in the hyperon and anti-hyperon rest frame, by using the 4-momentum conservation and perform a Lorentz transformation into the  $\bar{p}p$  centre of mass frame.

The schematic diagram of the kinematics of 4-Vector for all the particles in 3 different reference frame is illustrated in Figure 2.1 below.

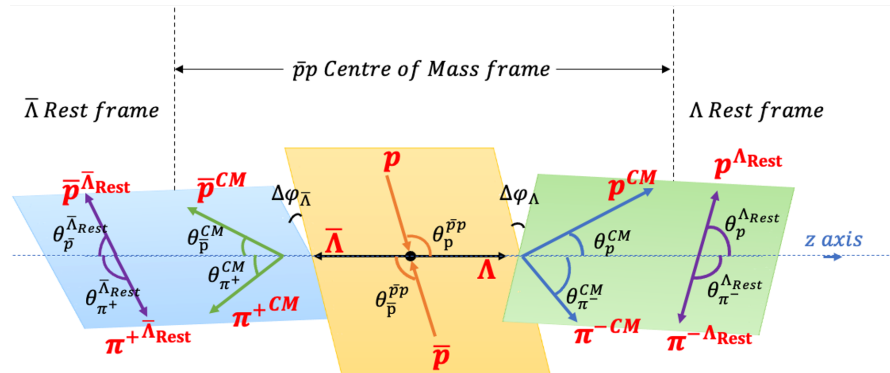


Figure 2.1: Schematic Diagram of the reaction in CM frame and Rest frame

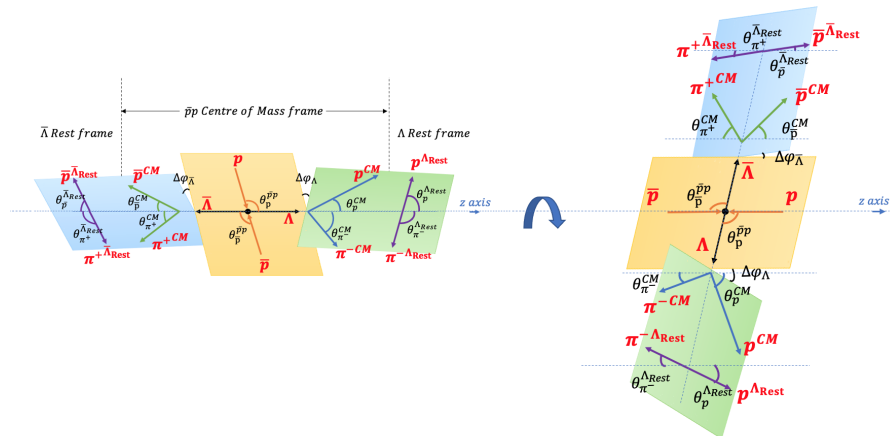


Figure 2.2: Schematic Diagram of the reaction in CM frame and Rest frame after rotation to align beam of antiproton to z-axis

The coordinate systems used in this report are defined in this way:

1. Before rotation (see section 2.3.2) and referring to figure 2.1:

The z-axis is in the direction along the  $\Lambda$  hyperon, the x-axis is at the direction that perpendicular to the  $\Lambda\bar{\Lambda}$  pair in the horizontal plane, and lastly the y-axis is the at the direction that perpendicular to the  $\Lambda\bar{\Lambda}$  pair in the vertical plane.

2. After rotation (see section 2.3.2) and referring to figure 2.2 :

The z-axis is changed to be in the direction along the antiproton beam, and the definition of x-axis and y-axis is similar to before rotation case, but they are perpendicular to the beam, in horizontal plane, and vertical plane, respectively.

It is called the helicity frame, which is commonly used when one studying the spin observable of polarisation for hyperon decays. And it is based on the helicity formalism (see, e.g., [4] and [15], for details about this formalism in the spin observable measurement in antihyperon-hyperon production at PANDA at FAIR).

We determine the centre of mass energy based on the assumption that we have a  $\bar{p}$  beam with 1.64 GeV/c beam momentum in lab system and a stationary  $p$  target. This will allow us to calculate the  $\Lambda\bar{\Lambda}$  final state momentum. In the actual simulation of our external event generator, we here start with generating isotropic distributions for the intermediate and final state particles.

## 2.1 4-Vector Kinematics

In the natural unit ( $\hbar = c = 1$ ), the 4-momentum  $P_\mu$  can be written as

$$P_\mu = \begin{pmatrix} E \\ p_x \\ p_y \\ p_z \end{pmatrix} \quad (2.1)$$

where  $E$  is the energy, while  $p_x, p_y$ , and  $p_z$  are the 3 dimensional component of the traditional momentum vector. The square of a 4-momentum, e.g.,  $P_A^2$ , satisfies the energy-momentum relation, and gives a Lorentz invariant quantity called invariant mass. The square of the 4-momentum  $P_A^2$  can be written as

$$P_A^2 \equiv E_A^2 - \vec{p}_A^2 = m_A^2 \quad (2.2)$$

where  $\vec{p}$  is the traditional 3 momentum vector. and  $m$  is the invariant mass. In the case of a scattering process of two particles into two particles, e.g.,  $A + B \rightarrow C + D$  their four-momentum conserve:  $P_A + P_B = P_C + P_D$ , they can then be written explicitly as

$$\begin{pmatrix} E_A \\ p_{A_x} \\ p_{A_y} \\ p_{A_z} \end{pmatrix} + \begin{pmatrix} E_B \\ p_{B_x} \\ p_{B_y} \\ p_{B_z} \end{pmatrix} = \begin{pmatrix} E_C \\ p_{C_x} \\ p_{C_y} \\ p_{C_z} \end{pmatrix} + \begin{pmatrix} E_D \\ p_{D_x} \\ p_{D_y} \\ p_{D_z} \end{pmatrix} \quad (2.3)$$

Now we consider the decay of a mother particle with mass  $M$  to two daughter particles of mass  $m_1$  and  $m_2$  in the rest frame of the parent particle. This implies  $P_1^2 = m_1^2$  and  $P_2^2 = m_2^2$ . By the 3-momentum conservation, the two daughter particles must be emitted back to back in the parent rest frame , we can choose the parameters to be two angles  $\theta$  and  $\varphi$  (polar angle and azimuth angle) defining the direction of one of the daughters. The 4-momentum of mother particle  $P$  satisfies the 4-momentum conservation,  $P = P_1 + P_2$  in parent's rest frame, and thus  $P = (M, \vec{0})$ . Rewriting  $P_2 = P - P_1$ , we get

$$P_2^2 = (P - P_1)^2 = P^2 - 2P \cdot P_1 + P_1^2 \quad (2.4)$$

and the mass

$$m_2^2 = M^2 - 2ME_1 + m_1^2 \quad (2.5)$$

The energy of the daughter particles can be written as

$$E_1 = \frac{M^2 + m_1^2 - m_2^2}{2M} \quad (2.6)$$

Using the relation of  $E_2 = M - E_1$ , in this case in parent's rest frame, and one obtains

$$E_2 = \frac{M^2 + m_2^2 - m_1^2}{2M} \quad (2.7)$$

Use the momentum form  $|\vec{p}_1| = \sqrt{E_1^2 - m_1^2}$  and one obtains

$$|\vec{p}_1| = \frac{\sqrt{(M^2 + m_1^2 - m_2^2)^2 - 4M^2m_1^2}}{2M} = \frac{\sqrt{(M^2 - m_1^2 - m_2^2)^2 - 4m_1^2m_2^2}}{2M} \quad (2.8)$$

Notice that it is symmetric under the interchange of daughter particle 1 and 2. Therefore, it would be an identical result and thus  $|\vec{p}_1| = |\vec{p}_2|$ , as we expected from the conservation of 3-momentum.

## 2.2 Hyperon and Anti-hyperon Rest Frame

The final states of particles are in these two frames. The absolute momentum  $|\vec{p}|$  of  $p\pi^-$  and  $\bar{p}\pi^+$  can be calculated from, e.g., equation (2.7). We begin with an isotropic emission profile, i.e., the distributions for  $\cos(\theta)$  and  $\varphi$  will be uniform. The above 4-momentum relation calculations are then all performed and stored in ROOT.

## 2.3 $\bar{p}p$ Centre of Mass Frame

Refer to Figure 2.1 again. The final state particles of the  $\bar{\Lambda}$  or  $\Lambda$  decays are generated, including the polar angle  $\theta$  and the azimuth angle  $\varphi$ . From the  $|\vec{p}|$ ,  $\theta$ , and  $\varphi$ , one can also obtain the components of momentum vector, i.e.,  $p_x, p_y, p_z$ . The next step is to transform the particles in the centre-of-mass (CM) system.

### 2.3.1 Lorentz Boost

The transformation of the particles into the CM frame is done using a Lorentz boost. We take the example of  $\Lambda \rightarrow p\pi^-$  to illustrate the calculation. Consider that the  $\Lambda$  is moving along the  $+z$  direction and assume the decay happens in the  $x$ - $z$  plane with  $\vec{p}_p$  being the proton momenta. Recall that the  $z$ -axis is along the  $\Lambda$  hyperon and is illustrated in the Figure 2.1, while the  $x$ -axis is perpendicular to  $z$ -axis according to Figure 2.1.

Using the results of Section 2.1 to apply the Lorentz boost in the  $\Lambda$  rest frame, and obtained

$$\begin{cases} |\vec{p}_{p_x}^*| = |\vec{p}_p^*| \sin\theta^* \\ |\vec{p}_{p_z}^*| = |\vec{p}_p^*| \cos\theta^* \end{cases} \quad (2.9)$$

Similarly we have

$$\begin{cases} |\vec{p}_{\pi_x^-}^*| = -|\vec{p}_{p_x}^*| \\ |\vec{p}_{\pi_z^-}^*| = -|\vec{p}_{p_z}^*| \end{cases} \quad (2.10)$$

While the energy of them can also be found

$$\begin{cases} E_p^* = \frac{m_\Lambda^2 + m_p^2 - m_\pi^2}{2m_\Lambda} \\ E_\pi^* = m_\Lambda - E_p^* \end{cases} \quad (2.11)$$

Where the quantity with upper asterisk (\*) symbol denotes the value in original mother particle rest frame.

The total energy of the  $\Lambda$  is given by

$$E_\Lambda = \sqrt{\vec{p}_\Lambda^2 + m_\Lambda^2} \quad (2.12)$$

This leads to the  $\gamma$  factor and the magnitude of velocity

$$\gamma_\Lambda = \frac{E_\Lambda}{m_\Lambda} \quad (2.13)$$

$$v_\Lambda = \frac{|\vec{p}_\Lambda|}{E_\Lambda} \quad (2.14)$$

The Lorentz transformation (LT) can be done by multiplying the factors we got above

$$\begin{cases} |\vec{p}_{p_x}| = |\vec{p}_{p_x}^*| \\ |\vec{p}_{p_z}| = \gamma_\Lambda (|\vec{p}_{p_z}^*| + v_\Lambda E_p^*) \\ \tan\theta_p = \frac{|\vec{p}_{p_x}|}{|\vec{p}_{p_z}|} \end{cases} \quad (2.15)$$

And similarly for the other daughter particle

$$\begin{cases} |\vec{p}_{\pi_x^-}| = |\vec{p}_{\pi_x^-}^*| \\ |\vec{p}_{\pi_z^-}| = \gamma_\Lambda (|\vec{p}_{\pi_z^-}^*| + v_\Lambda E_{\pi^-}) \\ \tan\theta_{\pi^-} = \frac{|\vec{p}_{\pi_x^-}|}{|\vec{p}_{\pi_z^-}|} \end{cases} \quad (2.16)$$

The updated new angles  $\theta_p$  and  $\theta_{\pi^-}$  are calculated from applying the LT relation. The hyperon side is presented as an example above, and it is the same principle that is applied for the antihyperon side, which generated new angles of  $\theta_{\bar{p}}$  and  $\theta_{\pi^+}$ , for which we assume the angular distribution in the final state for each side to be generated independently.

### 2.3.2 Rotation

Since it is common to align the beam and target particles in the z-axis for the convenience of setting and calculation, the orientation of the 4-vector we generated in previous step have to be rotated. To that end, all the 4-vectors of the intermediate and final state particles will be rotated until the z-axis aligns with beam direction, as shown in Figure 2.2.

To perform the rotation, the relation of angles in spherical coordinates

$$\begin{cases} x = r \cos\varphi \sin\theta \\ y = r \sin\varphi \sin\theta \\ z = r \cos\theta \end{cases} \quad (2.17)$$

where  $\theta$  is the angle represented the sum of two previous non-rotated angles after the rotation. It is defined as  $\theta = \theta_\Lambda + \theta_p$  or  $\theta = \theta_{\bar{\Lambda}} - \theta_{\bar{p}}$ , respectively.

The rotation operation can also be performed by the rotation matrices

$$R_x = \begin{pmatrix} 1 & 0 & 0 \\ 0 & \cos\theta & -\sin\theta \\ 0 & \sin\theta & \cos\theta \end{pmatrix} \quad (2.18)$$

$$R_y = \begin{pmatrix} \cos\theta & 0 & \sin\theta \\ 0 & 1 & 0 \\ -\sin\theta & 0 & \cos\theta \end{pmatrix} \quad (2.19)$$

$$R_z = \begin{pmatrix} \cos\theta & -\sin\theta & 0 \\ \sin\theta & \cos\theta & 0 \\ 0 & 0 & 1 \end{pmatrix} \quad (2.20)$$

And combine them all for a general situation

$$R = R_z(\alpha)R_y(\beta)R_x(\gamma) \quad (2.21)$$

where  $\alpha, \beta, \text{and } \gamma$  are arbitrary angles in a general rotation, measured from the axis of  $z, y$ , and  $x$  in the 3 dimensional spatial coordinates. Using these relations in spherical coordinates and one can do the rotation for both  $\theta$  and  $\varphi$  in the point of view when beam and target particle is in the  $z$ -axis as shown in the right-half of the Figure 2.2.

### 3 The framework and output results of the External Event Generator

In this chapter, using the corresponding methodology and physics relations presented in chapter 2, the idea, progress, and results of this external event generator that demonstrated in the reaction  $\bar{p}p \rightarrow \bar{\Lambda}\Lambda \rightarrow \bar{p}\pi^+ + p\pi^-$  is discussed.

$m_\Lambda$	$m_p$	$m_{\pi^-}$	$p_{beam}$
1.115 GeV/c <sup>2</sup>	0.9383 GeV/c <sup>2</sup>	0.1396 GeV/c <sup>2</sup>	1.64 GeV/c

Table 3.1: Mass of  $\Lambda$ , mass of proton, and mass of  $\pi^-$ , also the momentum of beam  $\bar{p}$  in  $\bar{p}p$  lab frame, they are all as input in the generator

Table 3.1 lists the input parameters: mass of  $\Lambda$  (same as  $\bar{\Lambda}$ ), proton (same as antiproton),  $\pi^-$  (same as  $\pi^+$ ) and beam momentum in  $\bar{p}p$  lab frame. They are used for calculation in the external event generator. The ROOT macro C++ file "TestLbarLGen.cpp" \* is developed, that can be run in ROOT and output a root file, can be considered as the output event file from the external event generator.

#### 3.1 ROOT Tree format

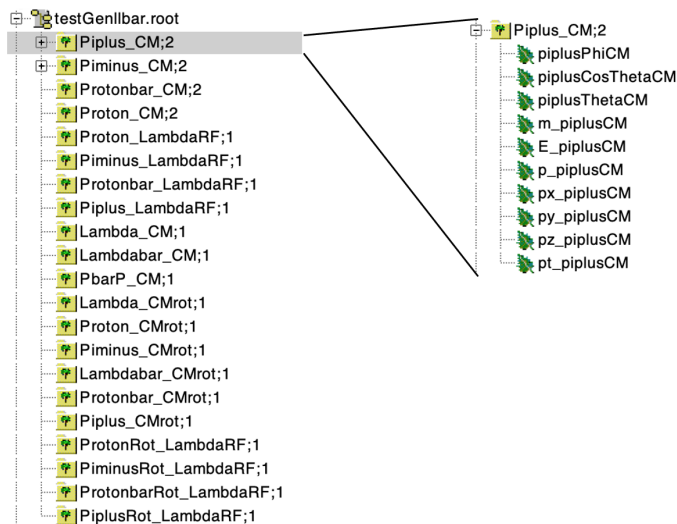


Figure 3.1: The output of root tree format file of the external event generator

\*The latest update of ROOT macro file can be found publicly on my GitHub, at this url:  
[https://github.com/shenvitor/lbar\\_EventGenerator](https://github.com/shenvitor/lbar_EventGenerator)

The output of the event generator is a root file named "testGenLbar.root", illustrated in Figure 3.1, which is created by a root macro file named "TestLbarLGen.cpp" that I have developed. The coding for running in the ROOT framework is based on the general idea and method introduced in chapter 2. And the tree section's naming is according to the particle's name and the reference frame that it belongs to.

- In the hyperon rest frame:  
"Proton\_LambdaRF" and "Piminus\_LambdaRF"
- In the anti-hyperon rest frame:  
"Protonbar\_LambdaRF" and "Piplus\_LambdaRF"
- In the CM frame of  $\bar{p}p$  system:  
"Proton\_CM", "Piminus\_CM",  
"Protonbar\_CM", "Piplus\_CM",  
"Lambda\_CM", "Lambdabar\_CM",  
and "PbarP\_CM" that storage the random angles of the beam in the CM frame.

Finally, the rotated particles are denoted with "Rot" or "rot":

- the hyperon rest frame after rotation  
"ProtonRot\_LambdaRF", "PiminusRot\_LambdaRF"
- the anti-hyperon rest frame after rotation  
"ProtonbarRot\_LambdaRF", "PiplusRot\_LambdaRF"
- the CM frame after rotation  
"Proton\_CMrot", "Piminus\_CMrot", "Protonbar\_CMrot", "Piplus\_CMrot", "Lambda\_CMrot",  
and "Lambdabar\_CMrot"

For each tree section, there are some branches. The branches contain the corresponding physical quantities distribution for that particular tree section. Refer to Figure 3.1, there are distribution of  $\varphi$  angles, value of  $\text{Cos}(\theta)$ ,  $\theta$  angles, mass, energy, magnitude of momentum, x, y ,z component of momentum, and also transverse component of momentum.

In the following section of 3.2 and 3.3, the unit of degree ( $^{\circ}$ ) is used for  $\varphi$  and  $\theta$  angles in the figures.

### 3.2 Test for uniform distribution

At first, the distribution of  $\text{Cos}(\theta)$  and  $\varphi$  for the particles in hyperon and antihyperon rest frame is generated in uniform distribution (by using the TRandom3 generator class in ROOT), as shown in Figure 3.2.

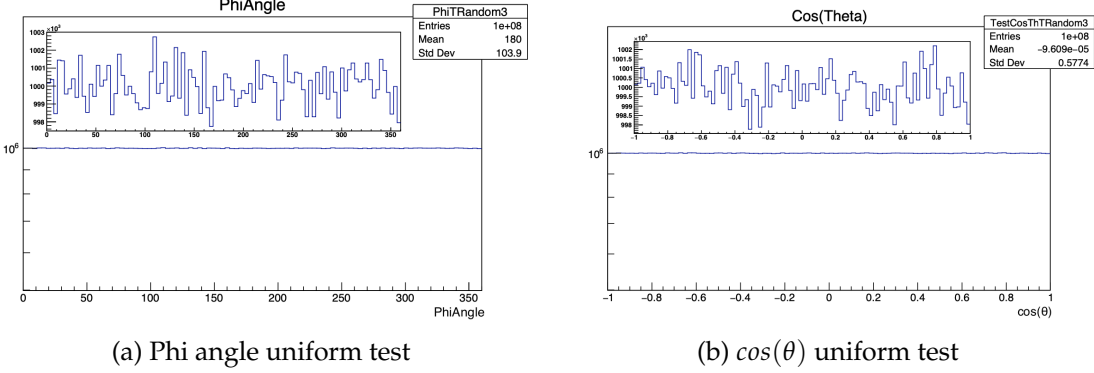


Figure 3.2: Testing the uniform distribution

This will produce the the distribution of  $\text{Cos}(\theta)$  and  $\varphi$  of the  $p\pi^-$  in  $\Lambda$  rest frame and the  $p\pi^+$  in  $\bar{\Lambda}$  rest frame.

The distribution of  $\text{Cos}(\theta)$  in the final state particles that we produced is uniform. Since an isotropic distribution of decay particles is considered here, and an isotropic distribution is one which is uniformly distributed in  $\text{Cos}(\theta)$ . This can be considered from the definition of the differential solid angle  $\Omega$ :

$$d\Omega = \frac{dA}{r^2} = \frac{2\pi r^2 \sin\theta d\theta}{r^2} = 2\pi \sin\theta d\theta = -2\pi d(\cos\theta) \quad (3.1)$$

Where A is the area, r is the radius, and  $\theta$  is the polar angle. It shows the linearity relations of the solid angle and value of  $\cos(\theta)$ ,

### 3.3 Generation of physics quantities

We shall focus on and check the generated distribution of angles for all the particle in  $\bar{p}p \rightarrow \bar{\Lambda}\Lambda \rightarrow p\pi^- + \bar{p}\pi^+$  in hyperon and antihyperon rest frame, then CM frame of  $\bar{p}p$  after Lorentz boost, and finally the rotation of orientation for all of them.

The distribution of  $\varphi$ ,  $\cos\theta$ , and  $\theta$  of different particles in various reference frame is presented in this section.

#### 3.3.1 Angular distribution in hyperon and antihyperon rest frame

Referring to Figure 3.3 and 3.4. In the rest frame of  $\Lambda$  and  $\bar{\Lambda}$ , for the production particles of  $p\pi^-$  and  $\bar{p}\pi^+$ , these quantities of uniform distribution of angle  $\varphi$  and value of  $\cos\theta$  are first generated independently.

That is also the case in the following presented results of generation. From left to right, the first column is the angle  $\varphi$ , the second column is the  $\cos\theta$ , and the third column is the  $\theta$  angle.

Also notice that, the isotropic setting of  $\varphi$  angle here will not be affected here after the Lorentz transformation and rotation, it is kept for checking it remains isotropic to verify the validity of the generation. But these are kept as the record, for the development of further possible extend of this project. When using a different model and assumption in the future studies, this can be changing.

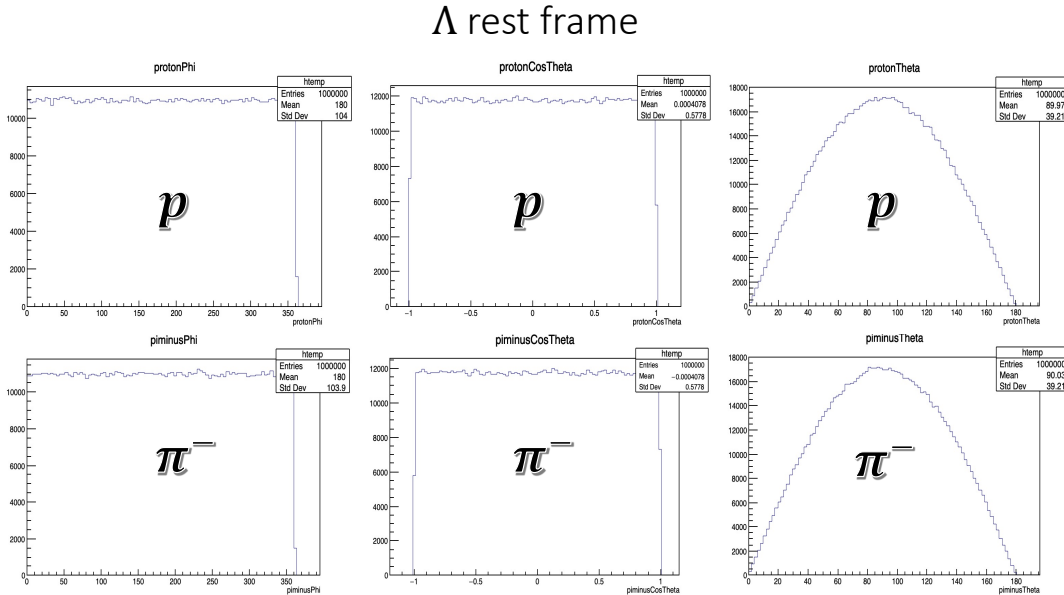


Figure 3.3: The distribution of  $\varphi$ ,  $\cos\theta$ , and  $\theta$  of  $p$  and  $\pi^-$  at hyperon rest frame

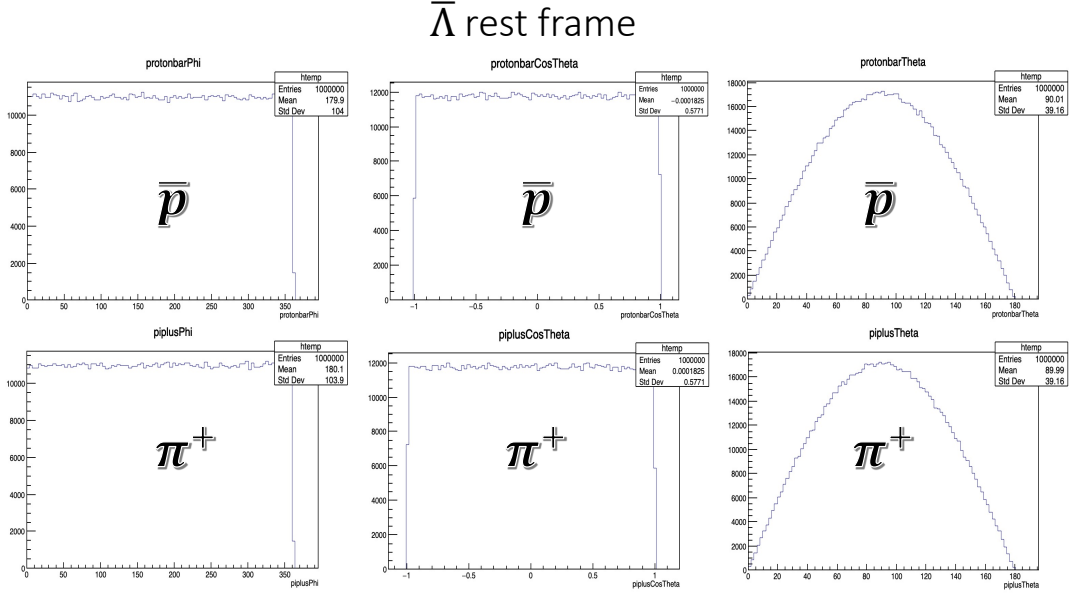


Figure 3.4: The distribution of  $\varphi$ ,  $\cos\theta$ , and  $\theta$  of  $\bar{p}$  and  $\pi^+$  at antihyperon rest frame

### 3.3.2 Angular distribution in $\bar{p}p$ CM frame

While the distribution of  $\varphi$  angle is also kept for the record of consistency check, the focus here is to look for the distribution of  $\cos\theta$  (or  $\theta$  equivalently), from the setting desired distribution (uniform at hyperon rest frame in this case) to the Lorentz transformed frame and rotation to beam aligned frame.

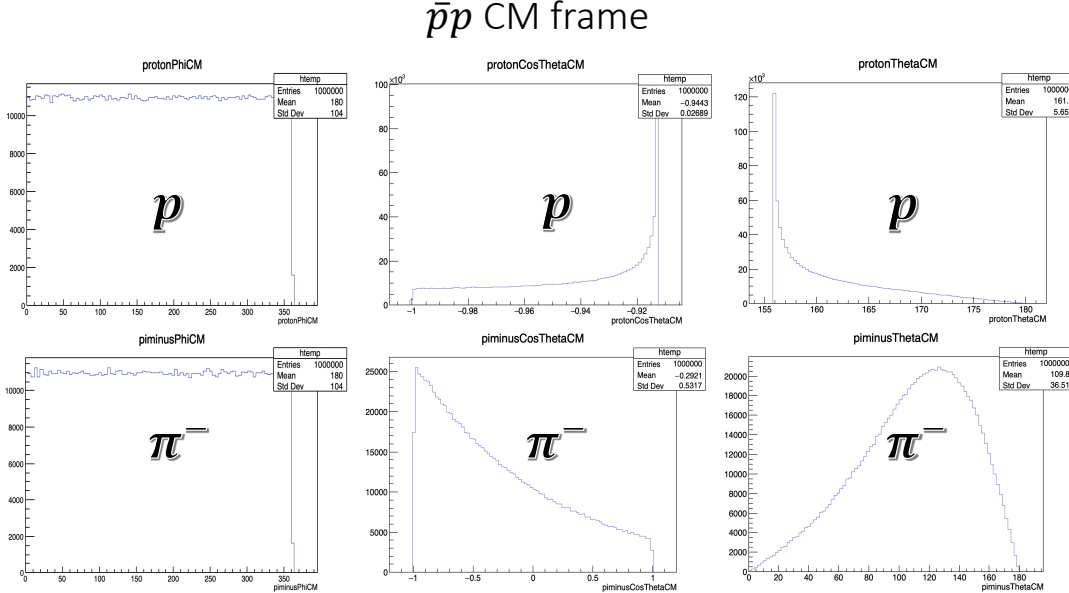


Figure 3.5: The distribution of  $\varphi$ ,  $\cos\theta$ , and  $\theta$  of  $p$  and  $\pi^-$  at  $\bar{p}p$  CM frame

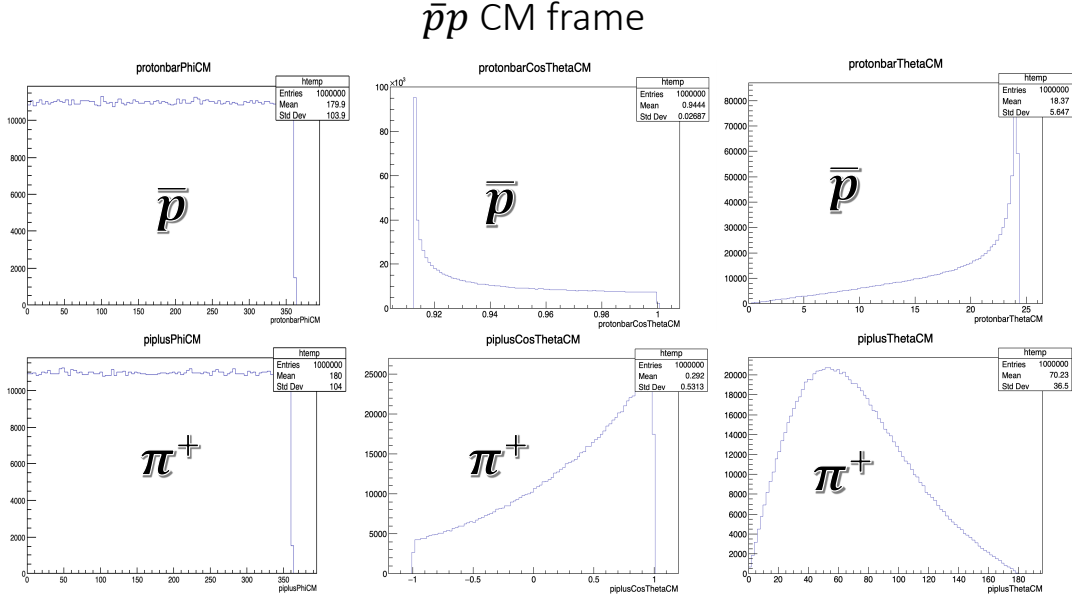


Figure 3.6: The distribution of  $\varphi$ ,  $\cos\theta$ , and  $\theta$  of  $\bar{p}$  and  $\pi^+$  at  $\bar{p}p$  CM frame

Referring to Figure 3.5 and 3.6. They are showing the distribution after the Lorentz boost to centre of mass frame of  $p\bar{p}$ . The principles of 4-vector conservation, the invariant mass, and the Lorentz boost relations, which is discussed in chapter 2, had been applied for developing and calculation in this part.

One can see in Figure 3.5 and 3.6 that after the boost their  $\theta$  distribution is non-symmetrical, in 2 different side of closer to  $0^\circ$  and  $180^\circ$ , or anti-hyperon side and hyperon side. Recall the mass of proton and pion, are 0.9383 GeV and 0.1396GeV, respectively. The proton is heavier than the pion (similarly for their anti-particles). As the result, the  $\theta$  angular distribution for the heavier one, proton, is emitting in a smaller coverage of angle  $\sim 25^\circ$  at this frame. Compare to the results of proton, the  $\theta$  angular distribution of pion is certainly emitting in a larger coverage of angles in almost all  $180^\circ$ , but preferred at the forward angles w.r.t. the emitting direction of their mother particle at this frame.

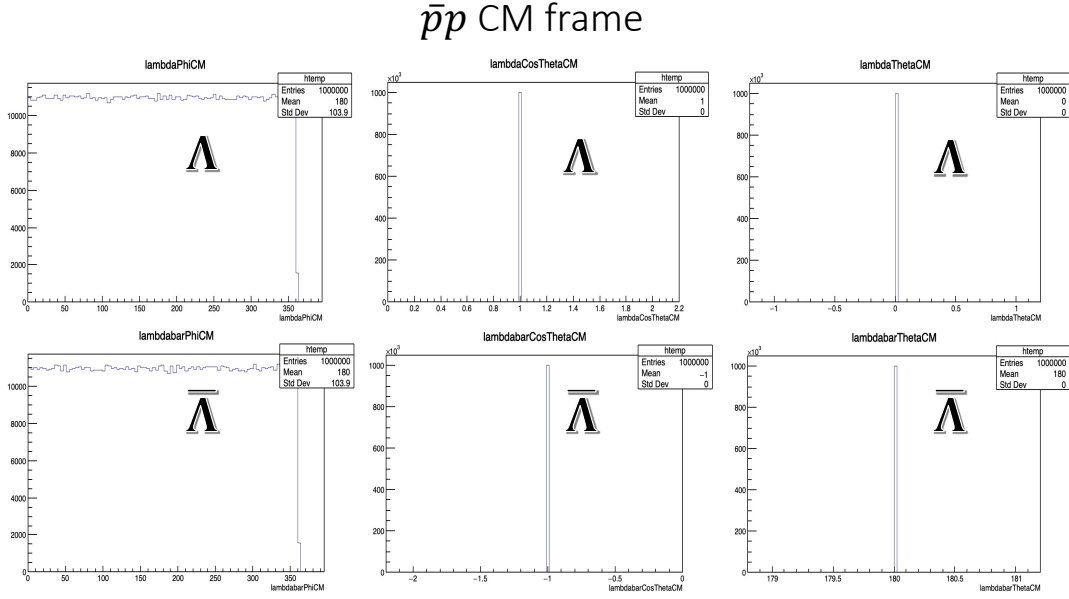


Figure 3.7: The distribution of  $\varphi$ ,  $\cos\theta$ , and  $\theta$  of  $\Lambda$  and  $\bar{\Lambda}$  at  $\bar{p}p$  CM frame

Referring to Figure 3.7 above. That is the antihyperon-hyperon pair,  $\bar{\Lambda}\Lambda$ , in the CM frame. As we introduce in the chapter 2, we assume initially the generation of them are align with the z-axis, thus we can notice their  $\cos\theta$  value are 1 and -1, respectively.

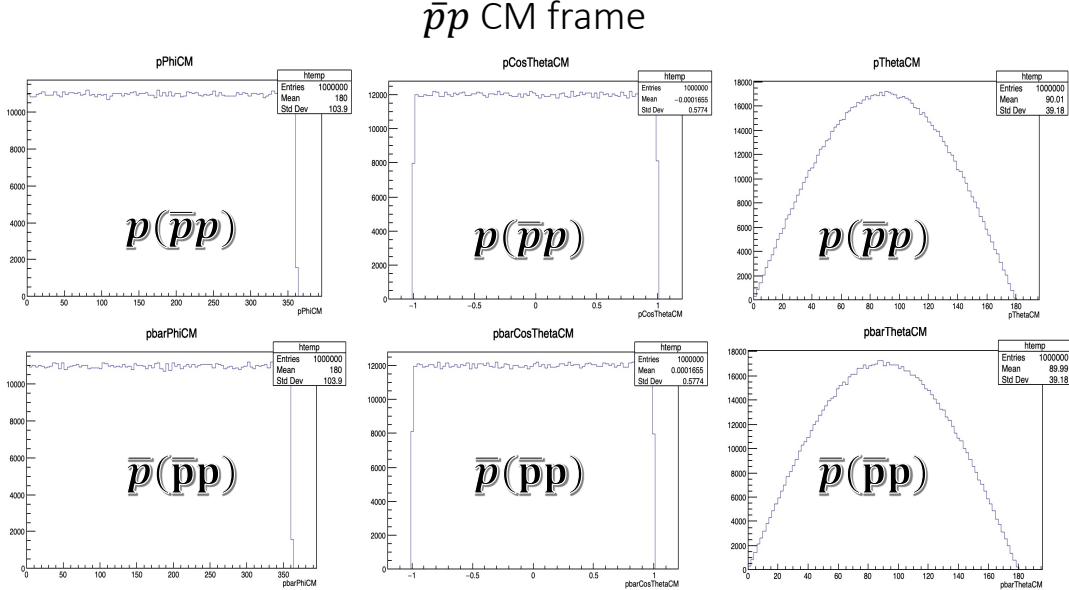


Figure 3.8: The distribution of  $\varphi$ ,  $\cos\theta$ , and  $\theta$  of  $\bar{p}p$  at  $\bar{p}p$  CM frame

Referring to Figure 3.8 above. The distribution of angles for the beam and target,  $\bar{p}p$ , are also needed to generate. Since these values of distribution, are later use for the rotation that for having the orientation of beam-target align with z-axis.

### 3.3.3 Angular distribution in $\bar{p}p$ CM frame after rotation

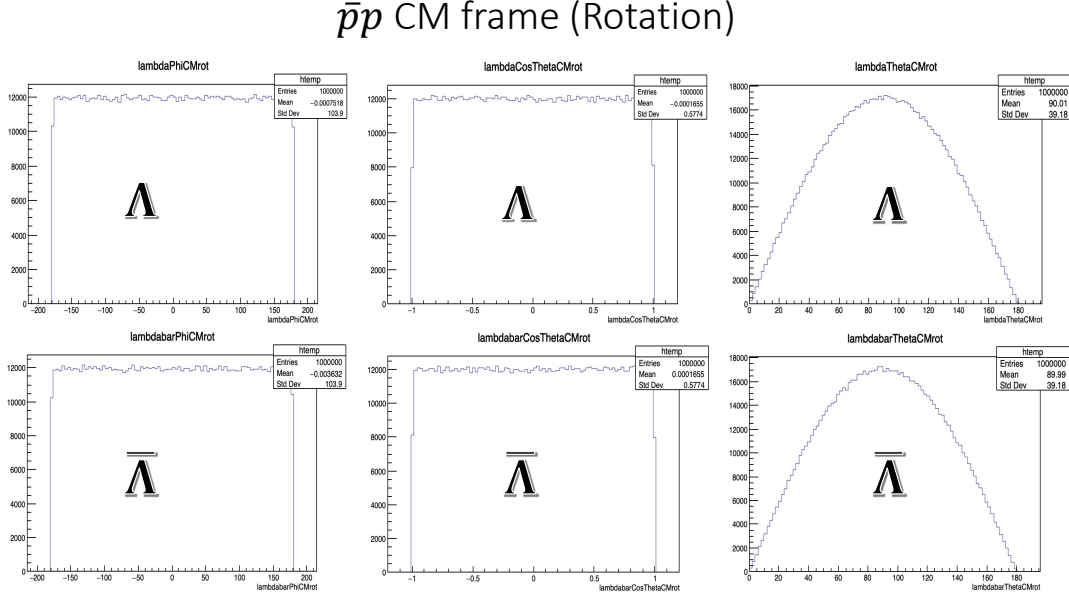


Figure 3.9: The distribution of  $\varphi$ ,  $\cos\theta$ , and  $\theta$  of  $\Lambda$  and  $\bar{\Lambda}$  at  $\bar{p}p$  CM frame after the rotation

Referring to Figure 3.9. As expected, it is the isotropic results are given out. It shows the result of distribution after applying the rotation from the distribution of figure 3.8 to distribution of figure 3.7, and thus for rotation of the  $\bar{\Lambda}\Lambda$ .

The Figure 3.10 and 3.11 below give the results of distribution of daughter particles in  $\bar{p}p$  Centre of Mass frame after the rotation in 3 dimensional space.

The values of  $\cos\theta$  distribution here of all of the daughter particles in the CM frame after rotation are in uniform. This implies the angular distribution in CM frame after Lorentz boost were somehow wash-out by this rotation transformation, and reverted to uniform distribution in this frame.

### $\bar{p}p$ CM frame (Rotation)

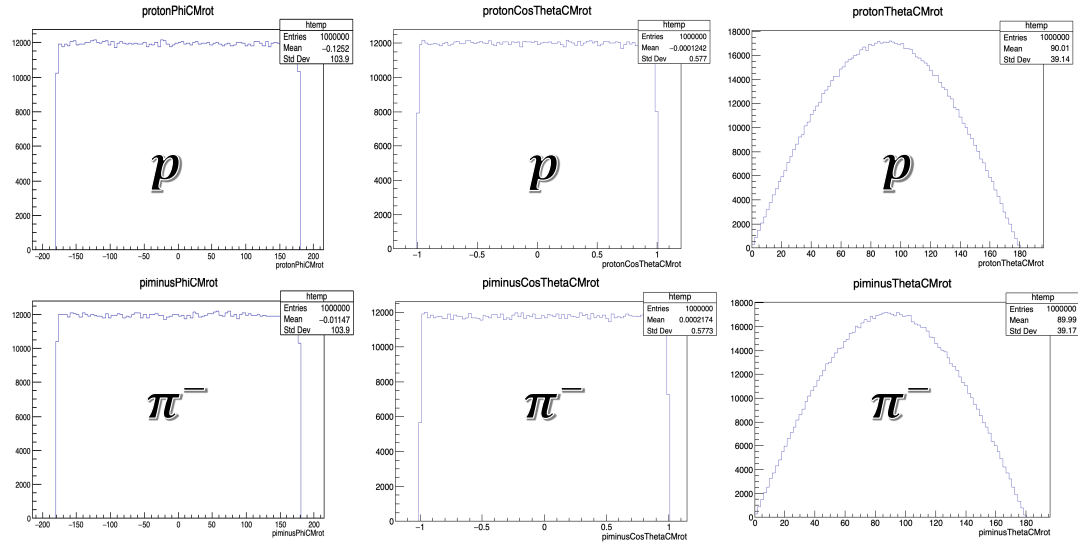


Figure 3.10: The distribution of  $\varphi$ ,  $\cos\theta$ , and  $\theta$  of  $p$  and  $\pi^-$  at  $\bar{p}p$  CM frame after the rotation

### $\bar{p}p$ CM frame (Rotation)

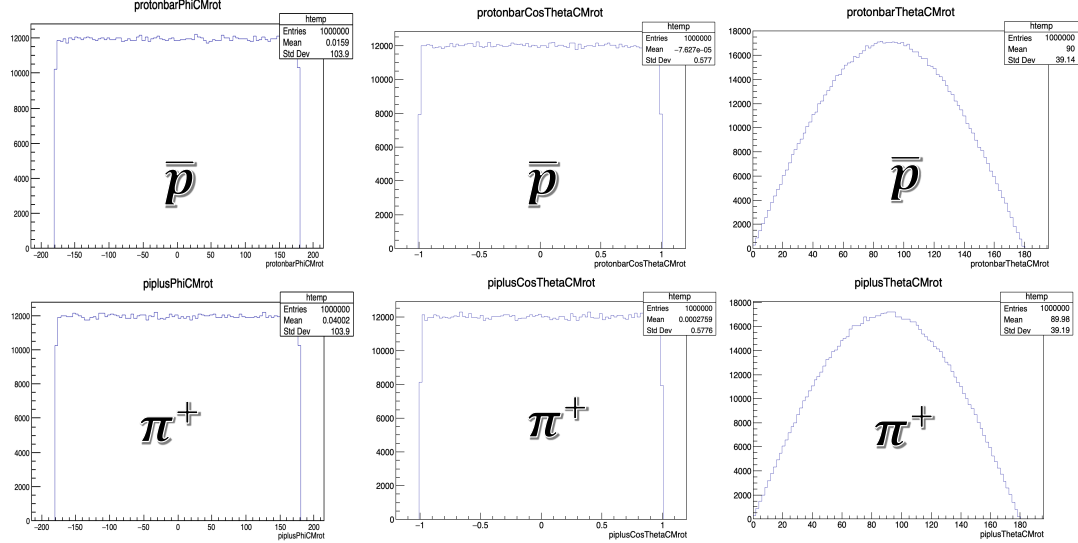


Figure 3.11: The distribution of  $\varphi$ ,  $\cos\theta$ , and  $\theta$  of  $\bar{p}$  and  $\pi^+$  at  $\bar{p}p$  CM frame after the rotation

### 3.3.4 Angular distribution in hyperon and antihyperon rest frame after rotation

Finally, referring to Figure 3.12 and 3.13. To transform to hyperon or antihyperon rest frame after rotation from the CM frame of  $\bar{p}p$  after rotation, the Lorentz boost in the other way around was applied, instead of directly rotate the angles in the hyperon rest frame as we did in the CM frame. Since the rotational angle that we generate is in the perspective of CM frame of  $\bar{p}p$  system, or the frame that  $\Lambda\bar{\Lambda}$  are moving, not the rest frame of  $\Lambda\bar{\Lambda}$ , and the rotational angles between CM frame of the system and rest frame of hyperon is not in a simply linearity relation. Thus, one should not directly use the same rotational angle in the CM frame and apply to the hyperon rest frame, to apply the Lorentz boost here back to hyperon rest frame is thus a easier strategy here.

We would expect the same distribution that was used in the beginning (the very first generation at hyperon and antihyperon rest frame). But here at the time of the end of this semester, my latest version of this event generator generates some different results of distribution (see figure 3.12 and 3.13), and was not able to produce the expected final stage of hyperon and antihyperon rest frame after rotation. Thus we assume there are still some kind of bugs in the transformation in this section 3.3.4 that still needed to be looked at it in the future. Yet everything performed by this generator before this section 3.3.4 seems reasonable at the moment, which means it is functioning well with some limitation discussed above.

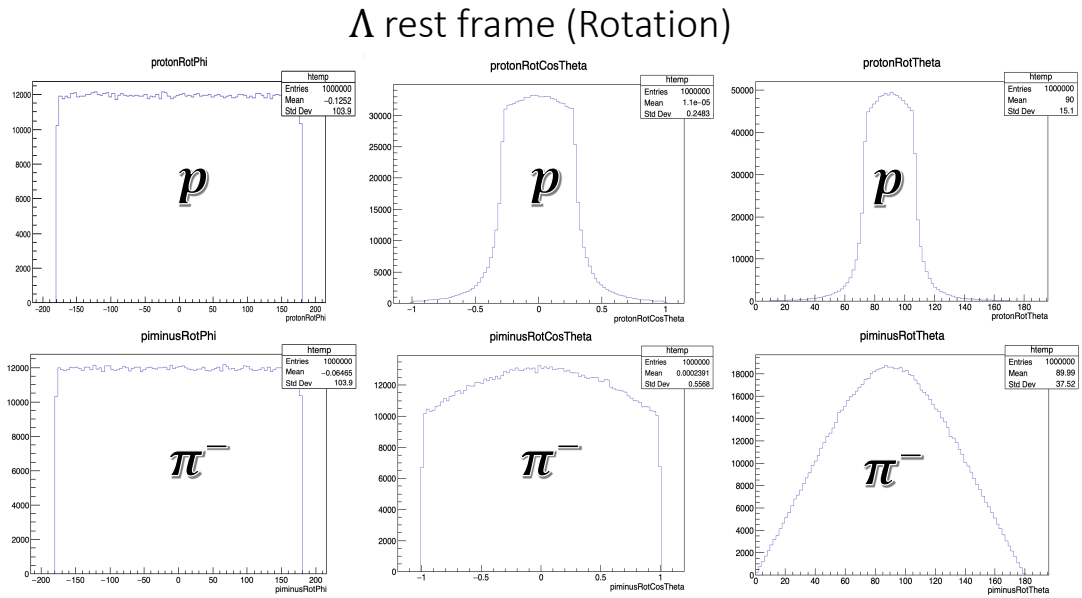


Figure 3.12: The distribution of  $\varphi$ ,  $\cos\theta$ , and  $\theta$  of  $p$  and  $\pi^-$  at hyperon rest frame after the rotation

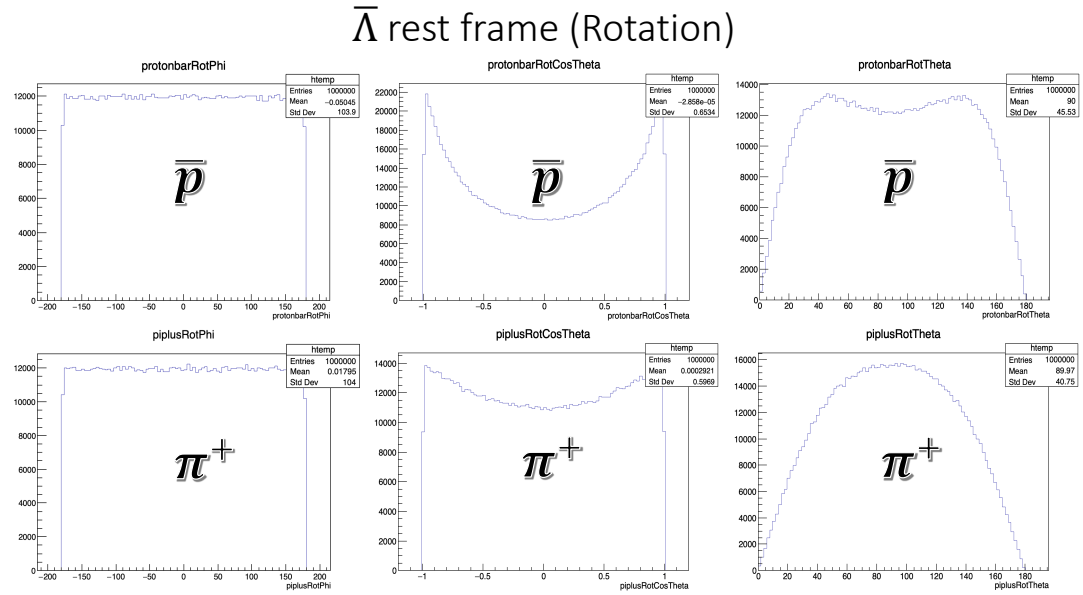


Figure 3.13: The distribution of  $\varphi$ ,  $\cos\theta$ , and  $\theta$  of  $\bar{p}$  and  $\pi^+$  at antihyperon rest frame after the rotation

## 4 Conclusion & Outlook

In this project report, a prototype of external Monte-Carlo Event Generator for the antihyperon-hyperon pair production in antiproton-proton annihilation, in particular for the reaction of  $\bar{p} + p \rightarrow \bar{\Lambda} + \Lambda \rightarrow \bar{p}\pi^+ + p\pi^-$ , based on their simplified kinematics relations of 4-vectors, is developed and presented.

This external MC event generator is built on ROOT, compare to embedded event generator used in PandaRoot, it can be more accessible and convenient to achieve the need of quickly testing models and formalisms about polarisation and spin-observables studies for antihyperon-hyperon pair production in antiproton-proton annihilation. To implement the desired distribution related to some testing models of spin-observables through the external event generator, with further studies and tests of the implementation, for example [16], [17] ,that we would want to investigate, would be the most probably future extension of this project.

Lastly, some features and future plans of this developing external MC event generator are pointed out below:

### # Features

- Beam momentum as input
- Fast MC simulation with light-weight software package
- Comprehensive set of angles and momentum in CM and helicity frame

### # Future plans

- Further development of distribution in CM and helicity frame after rotation
- Decay length to be added in the future
- Arbitrary angular distributions in the future

# Reference

- [1] PANDA Collaboration *et al.*, “PANDA Phase One: PANDA collaboration,” *European Physical Journal A*, vol. 57, no. 6, p. 184, 2021.
- [2] M. Durante, P. Indelicato, B. Jonson, V. Koch, K. Langanke, U.-G. Meißner, E. Nappi, T. Nilsson, T. Stöhlker, E. Widmann, *et al.*, “All the fun of the FAIR: Fundamental physics at the facility for antiproton and ion research,” *Physica Scripta*, vol. 94, no. 3, p. 033 001, 2019.
- [3] S. Spataro, “Event Reconstruction in the PandaRoot framework,” in *Journal of Physics: Conference Series*, IOP Publishing, vol. 396, 2012, p. 022 048.
- [4] M. Papenbrock, PANDA collaboration, *et al.*, “Spin observables in antihyperon-hyperon production at PANDA at FAIR,” in *Journal of Physics: Conference Series*, IOP Publishing, vol. 678, 2016, p. 012 019.
- [5] R. Brun and F. Rademakers, “ROOT—An object oriented data analysis framework,” *Nuclear instruments and methods in physics research section A: accelerators, spectrometers, detectors and associated equipment*, vol. 389, no. 1-2, pp. 81–86, 1997.
- [6] M. Al-Turany, D. Bertini, R. Karabowicz, D. Kresan, P. Malzacher, T. Stockmanns, and F. Uhlig, “The FairRoot framework,” in *Journal of Physics: Conference Series*, IOP Publishing, vol. 396, 2012, p. 022 001.
- [7] Particle Data Group, P. Zyla, R. Barnett, J. Beringer, O. Dahl, D. Dwyer, D. Groom, C.-J. Lin, K. Lugovsky, E. Pianori, *et al.*, “Review of particle physics,” *Progress of Theoretical and Experimental Physics*, vol. 2020, no. 8, p. 083C01, 2020.
- [8] D. Steinschaden, PANDA Collaboration, *et al.*, “Event Reconstruction and Simulation in PandaRoot for the PANDA experiment,” in *Journal of Physics: Conference Series*, IOP Publishing, vol. 1085, 2018, p. 042 045.
- [9] D. J. Lange, “The EvtGen particle decay simulation package,” *Nuclear Instruments and Methods in Physics Research Section A: Accelerators, Spectrometers, Detectors and Associated Equipment*, vol. 462, no. 1-2, pp. 152–155, 2001.
- [10] J. Sempau, S. J. Wilderman, and A. F. Bielajew, “DPM, a fast, accurate Monte Carlo code optimized for photon and electron radiotherapy treatment planning dose calculations,” *Physics in Medicine & Biology*, vol. 45, no. 8, p. 2263, 2000.

- [11] H. Petersen, M. Bleicher, S. A. Bass, and H. Stöcker, "UrQMD-2.3-Changes and Comparisons," *arXiv preprint arXiv:0805.0567*, 2008.
- [12] T. Sjöstrand, S. Ask, J. R. Christiansen, R. Corke, N. Desai, P. Ilten, S. Mrenna, S. Prestel, C. O. Rasmussen, and P. Z. Skands, "An introduction to PYTHIA 8.2," *Computer physics communications*, vol. 191, pp. 159–177, 2015.
- [13] S. Agostinelli, J. Allison, K. a. Amako, J. Apostolakis, H. Araujo, P. Arce, M. Asai, D. Axen, S. Banerjee, G. Barrand, *et al.*, "GEANT4—a simulation toolkit," *Nuclear instruments and methods in physics research section A: Accelerators, Spectrometers, Detectors and Associated Equipment*, vol. 506, no. 3, pp. 250–303, 2003.
- [14] R. Brun, A. McPherson, P. Zanarini, M. Maire, and F. Bruyant, "GEANT 3: User's guide Geant 3.10, Geant 3.11," CERN, Tech. Rep., 1987.
- [15] W. I. Andersson, "Future spin observables measurements with the PANDA detector at FAIR," in *Journal of Physics: Conference Series*, IOP Publishing, vol. 1667, 2020, p. 012014.
- [16] E. Perotti, G. Fäldt, A. Kupsc, S. Leupold, and J. J. Song, "Polarization observables in e+ e- annihilation to a baryon-antibaryon pair," *Physical Review D*, vol. 99, no. 5, p. 056 008, 2019.
- [17] PANDA Collaboration *et al.*, "The potential of  $\Lambda$  and  $\Xi^-$  studies with PANDA at FAIR," *arXiv preprint arXiv:2009.11582*, 2020.